Thermochimica Acta 472 (2008) 84–94

Contents lists available at ScienceDirect

Thermochimica Acta

journal homepage: www.elsevier.com/locate/tca

Conversion of the volatile thermal decomposition products of polyamide-6,6 and ABS over Y zeolites

János Bozi, Zsuzsanna Czégény, Marianne Blazsó*

Institute of Materials and Environmental Chemistry, Chemical Research Centre, Hungarian Academy of Sciences, H-1525, P.O. Box 17, Budapest, Hungary

ARTICLE INFO

Article history:
Received 29 February 2008
Accepted 31 March 2008
Available online 8 April 2008

Keywords:
Polyamide-6,6
ABS
Catalytic conversion
Y zeolite
TG–MS
Pyrolysis–GC/MS

ABSTRACT

Thermal decomposition products of polyamide-6,6 (PA-6,6) and acrylonitrile–butadiene–styrene copolymer (ABS) have been converted over Y zeolites at above the temperature of thermal decomposition of these polymers. On-line pyrolysis–gas chromatography/mass spectrometric (Py–GC/MS) analysis revealed the nature of chemical reactions of the pyrolysis gas and oil components taking place over protonic and sodium Y zeolite. Selected TG–MS ion curves of polymer and zeolite mixtures indicated the changes due to the catalytic conversion of the thermally produced products in to compounds of high volatility.

The experimental results demonstrate that protonic Y zeolite (HUSY and NH_4Y) denitrogenate the pyrolysis oil components and transform the hydrocarbon part of their molecules into aromatic compounds. Over sodium Y zeolite (NaY) pyrolysis product molecules of low volatility are cracked to gases and to compounds of gasoline volatility, but no denitrogenation occur. The aromatizing and hydrogenating activity of NaY zeolite is considerably lower, than that of protonic Y zeolites.

1. Introduction

Pyrolysis proved to be a suitable method for recycling plastic waste at temperature range of 400–800 °C [1,2]. Since thermal degradation of polymers often produces a broad product range and requires high operating temperature, catalytic pyrolysis was investigated as an alternative process solving these problems. A suitable catalyst can both control the nature of the products and reduce the reaction temperature. Among various commercial or laboratory prepared catalysts zeolite has been applied often [3–6], and most of the studies were confined to pure polymers or their mixtures predominantly polyolefin, polystyrene and rubber [4–10].

Waste electronic and electric equipments (WEEE), and automotive plastic shredder contain various nitrogen- and halogen-containing polymers and additives. The pyrolytic recycling of the plastics from such a complex waste generates several specific problems, because it involves the evolution of many environmentally hazardous compounds [11,12]. Two kinds of attempts are applicable for diminishing the concentration of inconvenient components in the pyrolysis oil of wastes: inhibition of their evolution on one hand and transforming or removing them from the pyrolysis oil on the other hand. Catalytic upgrading of pyrolysis oils obtained from plastics wastes also proved to be a convenient way to reduce broad volatility range and to convert components into valuable chemicals [13–16]. Analytical pyrolysis studies are reported on the catalytic conversion of pyrolysis products through direct coupling of the reactor output to GC/MS [13,16].

Polyamide-6,6 (PA-6,6) and acrylonitrile–butadiene–styrene copolymer (ABS) are frequently used nitrogen-containing polymers in electrical and electronic equipment and automobile. Thermal degradation – including mechanisms and product analysis – of these polymers have been extensively studied in the past few decades [17–23]. But only a few catalytic studies have been published on nitrogen-containing polymers [24,25], although catalytic hydrodenitrogenation (HDN) is already an industrially applicable process for reducing the level of nitrogen content in mineral feedstocks over supported Ni-Mo catalysts [26,27].

The purpose of this work was to study the conversion of pyrolysis gases and oils of two typical nitrogen-containing polymers over commercial zeolites of low cost. Pyrolysis–catalysis–GC/MS on-line analysis – a method developed in our laboratory [28] – has been applied for on-line separation and analysis of the volatile components of the catalytically converted pyrolysis products. In TG–MS measurements carried out additionally only a small part of the thermally evolved volatile products of polymer can get contacted with the added zeolite. Nevertheless, the detection of molecular ion intensities of the gases evolved in these experiments is sensitive enough for monitoring the changes due to the partial conversion of the thermally produced compounds in to gas products by the zeolite at above the temperature of polymer decomposition.

* Corresponding author. Tel.: +36 14381148; fax: +36 14381147.
E-mail address: blazso@chemres.hu (M. Blazsó).

0040-6031/$ – see front matter © 2008 Elsevier B.V. All rights reserved.
doi:10.1016/j.tca.2008.03.018

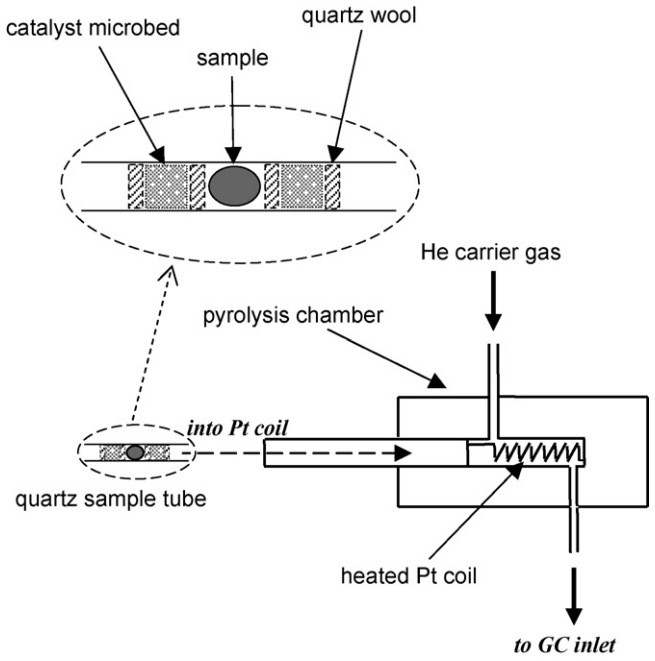

Fig. 1. Sample arrangement in the micropyrolyser for studying catalytic conversion of pyrolysis products.

2. Experimental

2.1. Materials

2.1.1. Nitrogen-containing polymers

Polyamide-6,6 (Nylon 6/6 pellets, melting point: 267 °C) and ABS [poly(acrylonitrile-*co*-butadiene-*co*-styrene, with acrylonitrile of ~25 wt.%, melting point: 110 °C)] contained no additives and were used as received from Sigma–Aldrich.

2.1.2. Catalysts

Zeolites used in this study were molecular sieve 4 Å (Fluka) sodium form with pore diameter 0.4 nm and of Si/Al = 1, Y zeolites with average pore diameter 0.74 nm, namely ultra stable hydrogen form of Si/Al = 2.49 (HUSY), ammonium–sodium form of Si/Al = 2.51 (NH_4NaY), and sodium form of Si/Al = 2.44 (NaY) (Grace Davison). Moreover, NH_4NaY was calcined at 450 °C for 3 h in nitrogen for obtaining a zeolite of mostly hydrogen form with minor sodium content (molar ratio of 4.6:1). The ion exchange capacity of the zeolite has been decreased by 17% due to calcination indicating partial dealumination resulting in a lower Brønsted acidity. The acidic properties of the original and calcined catalysts were determined by a conventional temperature programmed desorption (TPD) experiment.

2.2. Pyrolysis–catalysis–GC/MS

Pyrolysis–catalysis experiments were performed at 500 or 550 °C for 20 s in a Pyroprobe 2000 pyrolyser (Chemical Data System, USA) equipped with a platinum coil and quartz sample tube interfaced to a gas chromatograph (Agilent 6890) coupled with a mass selective detector (Agilent 5973). As Fig. 1 shows, two catalyst microbeds were placed at both ends into the sample holder quartz tube, making the pyrolysis vapour to pass through the catalyst heated at the same temperature as the sample. The catalyst bed was separated from the sample with quartz wool plugs in order to prevent direct contact of the catalyst particles and the polymer. Approximately 0.1–0.3 mg polymer sample was pyrolysed, the mass of the catalyst beds were 0.5–0.9 mg at both sides of the sample. Helium carrier gas at a flow rate of 20 mL min^{-1} purged the pyrolysis chamber held at 250 °C that was split prior to be introduced into the GC column. The GC separation was carried out on a HP-5MS capillary column (30 m × 0.25 mm × 0.25 μm, Agilent Technologies, USA). After 1 min of isotherm period at 50 °C the oven temperature was programmed to 300 °C at 10 °C min^{-1} heating rate and held at 300 °C for 4 min. The temperature of the transfer line of GC/MS and the source of the mass spectrometer were 280 and 200 °C, respectively. The mass spectrometer was operating in electron-impact mode (EI) at 70 eV. The spectra were obtained over a mass range of 14–450 Da. The GC/MS identification of pyrolysis products has been carried out by using mass spectral library, mass spectrometric identification principles and gas chromatographic retention relations. The relative standard deviation of GC/MS peak areas (related to unit sample mass) of the parallel experiments was about 3% and never exceeded 10% with careful sampling and properly heated transfer lines.

2.3. Thermogravimetry–mass spectrometry (TG–MS)

The TG–MS instrument was built from a PerkinElmer TGS-2 thermobalance and a Hiden HAL 3F/PIC mass spectrometer and controlled by a computer. The samples were heated at 10 °C min^{-1} up to 900 °C in a flowing argon atmosphere (140 ml min^{-1}). A portion of the volatile products was introduced into the ion source of the mass spectrometer through a glass lined metal capillary held at 300 °C. The quadrupole mass spectrometer was operated at 70 eV electron energy. The ion intensities were normalised to the sample mass and to the intensity of the ^{38}Ar isotope of the carrier gas. Since ammonia and water are evolving nearly simultaneously from PA 6,6 the molecular ion curves of ammonia at m/z 17 have been corrected taking into consideration the intensity of $[M-1]^+$ fragment ion of water molecule.

The catalyst powder of about 0.5 mg was covered by polymer powder of similar mass. The purpose of such sampling was to result in a good contact of catalyst with the melted polymer flowing down between the catalyst particles upon heating. The catalyst mass and any mass loss of it has been distracted from the total mass in the diagrams of the demonstrated TG analyses, so the residual mass does not involve the catalyst only the carbon deposit on it and the remains of the polymer after pyrolysis.

Kinetic parameters have not been calculated, because the subject of this work was not the thermal and catalytic decomposition of PA 6,6 and ABS, but the conversion of the volatile products over zeolites. TG curves were compared only to demonstrate the tendency of slight changes of the volatile evolution in the presence of various zeolites during the thermal decomposition of the polymers.

3. Results and discussion

The conversion of the volatile pyrolysis products of polymers was studied over Y type zeolites that are commercially available in various cationic forms such as hydrogen, ammonium and sodium. It is known that the ultrastabilization of HY zeolite by steaming results in lower Brønsted acidity and calcination may lead also to some dealumination without changing the Y zeolite structure under 600 °C [29]. In this way the variation of the converted product distribution over the studied catalysts may be understood on the basis of catalyzed reactions influenced by the nature and density of cations in the pores of Y zeolite. Nevertheless, in the multicomponent system of pyrolysis gas and oil it is hardly possible to

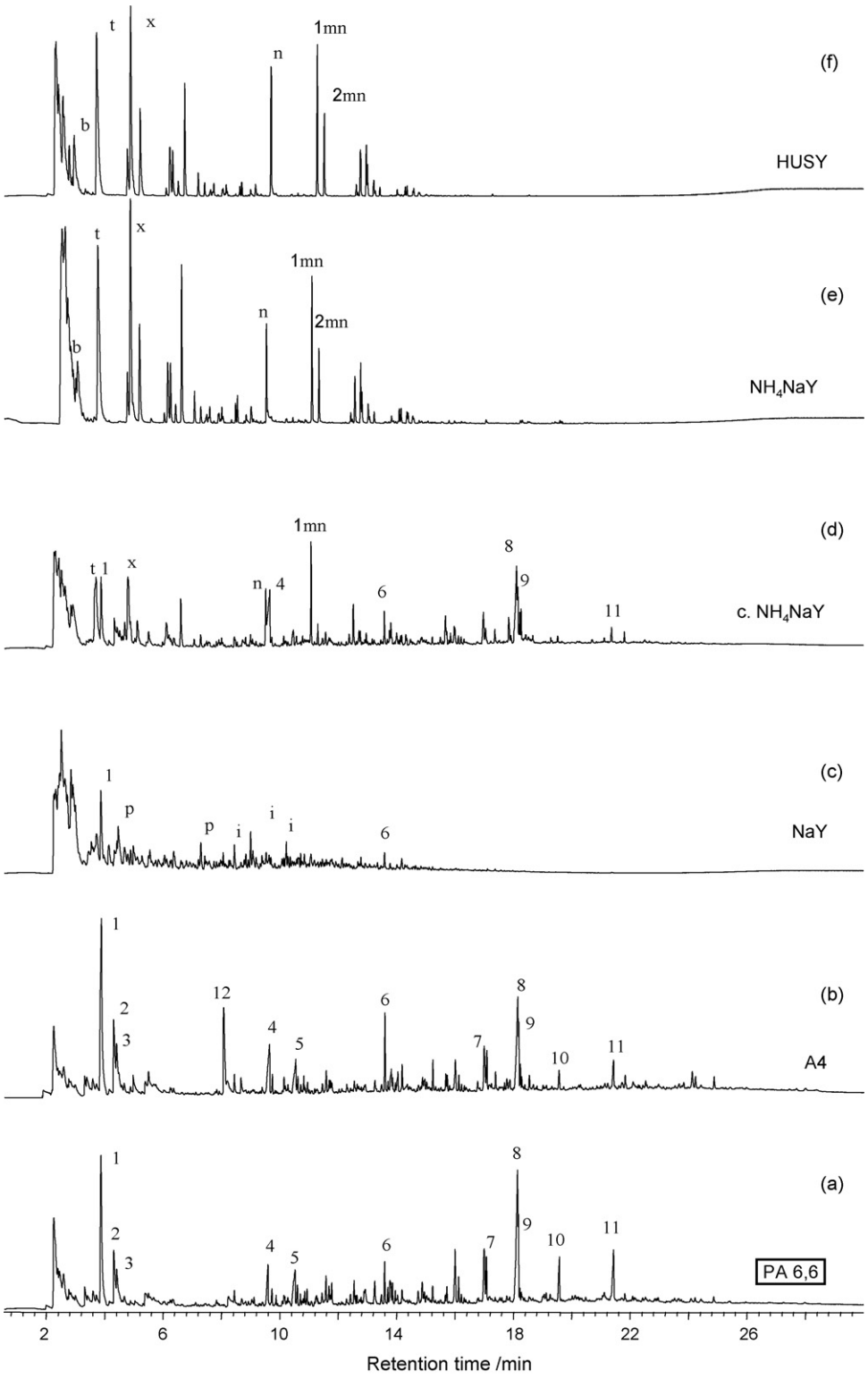

Fig. 2. Pyrolysis–gas chromatogram of PA-6,6 at 500 °C (a), and that obtained over microbed of molecular sieve 4A (b), of NaY (c), of calcined NH_4NaY (d), of NH_4NaY (e) and of HUSY (f) zeolites. The intensity range is the same (count/mg polymer) for all chromatograms. Peak annotation: b, benzene; t, toluene; x, *o*- and *p*-xylene; n, naphthalene; 1 mn, 1-methylnaphthalene; 2mn, 2-methylnaphthalene; p, nitroaromatic compounds; i, indanol and indenes; numbered peak identities are given in Table 1.

establish unambiguous correlation of the reactions taking place and the detailed zeolite structure such as location, strength, and ratio of Brønsted and Lewis acid sites.

Experiments with Molecular sieve 4A have been carried out in order to check the extent of the heat transfer limitation effect of solid catalyst among the experimental conditions at elevated temperature. No catalytic conversion is expected over this zeolite of narrow pore size because the pyrolysis product molecules are larger than the pores thus they cannot reach the cations in the inner surface of the pores.

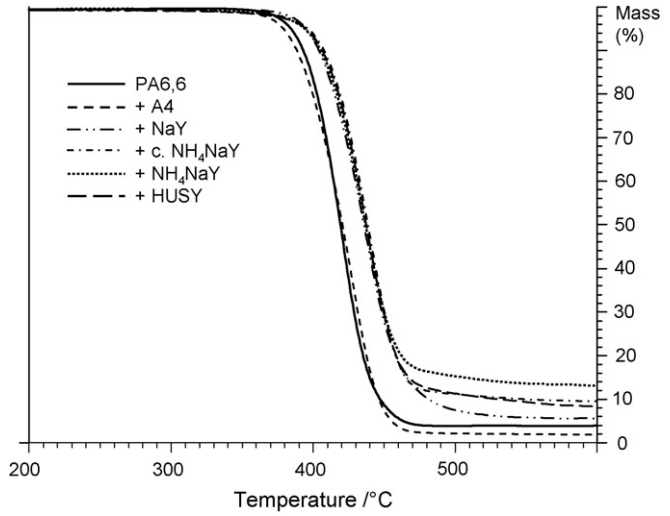

Fig. 3. Thermogravimetric analysis of PA-6,6 with zeolites. Mass loss curve of PA-6,6, full line; PA-6,6 with 4A, short dashed line; PA-6,6 with NaY, double dotted-dashed line; PA-6,6 with calcined NH_4NaY, dotted-dashed line; PA-6,6 with NH_4NaY, dotted line; PA-6,6 with HUSY, long dashed line.

3.1. Polyamide-6,6

Thermal decomposition of PA-6,6 leads cyclopentanone and a number of aliphatic nitrogen-containing compounds including amines, nitriles, acyclic and cyclic amides [17–21]. The total ion chromatogram of the pyrolysis products are shown in Fig. 2 together with those of the catalytically modified pyrolysates. The first unresolved peak covers gaseous and light volatile products such as carbon oxides, ammonia, water, light amines, nitriles and unsaturated hydrocarbons of 2–6 carbon atoms. The tentatively identified pyrolysis oil components are listed in Table 1. The structure and composition of these components are matching with the known thermal decomposition mechanism of PA-6,6 (shown in Scheme 1) via *cis*-elimination resulting in nitriles and amines, moreover cyclopentanone formation [17–20], and through intramolecular rearrangement of a pair of amide groups producing cyclic diamide and other oligomeric cycles [21]. TG curve displayed in Fig. 3 shows similar plot to published ones and indicates that this polymer starts to decompose to volatile products at around 370 °C when heated gradually in an inert atmosphere, and only a few percent of solid residue is left behind after pyrolysis completed at above 470 °C. Although only gases and highly volatile compounds can be detected due to the limitations of the TG–MS device, some useful information can be obtained on the reactions resulting in the detectable products. Ion profile of m/z 44 (molecular ion of CO_2) in Fig. 4a shows that carbon dioxide formation occurs in the first half of the PA-6,6 decomposition, most probably by decarboxylation of carboxyl groups either present as terminating groups or produced by hydrolysis. Ion curve of m/z 17 (molecular ion of NH_3) demonstrates that ammonia evolves at the highest rate in the middle of the mass loss of the polymer by elimination from primary amine products. *Cis*-elimination of amide group leads to imide that decomposes to nitrile by water loss in the main decomposition reaction (see Scheme 1) which could be traced by monitoring molecular ion of water at m/z 18. The characteristic fragment ion profile of volatile amines at m/z 30 follows the same plot as that of water, both compounds evolved at the highest rate in the centre of polyamide thermal destruction.

Table 1
Main thermal decomposition products of PA 6,6 at 500 °C

GC peak number[a]	Compound name	*M* (Da)	Retention time (min)
Gas[b]	Carbon dioxide[c]	44	1.79
1	Cyclopentanone[c]	84	3.43
2	Hex-5-enylamine[c]	99	3.89
3	1-Hexanamine[c]	101	3.99
4	Adiponitrile[c]	108	9.26
5	Caprolactam[c]	113	10.26
6	Trihydro-4-ethenylquinolin[d]	159	13.32
7	*N*-Pentyl-5-cyanopentanamide[d]	196	16.86
8	*N*-Hex-5-enyl-5-cyanopentanamide[d]	208	17.95
9	*N*-Hexyl-5-cyanopentanamide[d]	210	17.98
10	Dehydrated cyclic monomer of PA 6,6[d]	208	19.40
11	1,8-Diazacyclotetradecane-1,8-dihydro-2,7-Dione (cyclic monomer of PA 6,6)[d]	226	21.30

[a] Peak number refers to the indication in Fig. 2.
[b] Within the first unresolved peak in the total ion chromatogram in Fig. 2.
[c] Identified by MS library search.
[d] Tentatively identified.

3.1.1. Effect of molecular sieve 4A on the pyrolysis products of PA6,6

A new product (1,6-hexanediamine, peak 12) is observed in gas chromatogram b compared to a in Fig. 2. Moreover, a significant intensity raise of peaks 1–6 and a drop of peaks 10 and 11 are apparent also noticeable in Table 1. Presumably the observed effects are due to the outer surface of the 4A zeolite, since the pyrolysis product molecules cannot enter into the narrow pores of 0.4 nm. The diamine new product and the considerable increase of carbon dioxide evolution suggest that hydrolysis of amide groups is strongly promoted on the surface of this molecular sieve. The partial transformation of the cyclic amides of low volatility (peaks 10 and 11) can be also explained by their partial hydrolysis; moreover, the increased amount of the other lighter products could originate through hydrolysis from such large polyamide fragments that are not amenable by GC thus not appearing in the chromatogram of PA-6,6 pyrolysis products.

The TG–MS ion curve monitored at m/z 44 shown in Fig. 4b is considerably wider than the corresponding one in Fig. 4a indicating that – similar to the observations by pyrolysis–GC/MS – significantly more carbon dioxide is evolved in the experiment with 4A than from PA-6,6 alone. This observation confirms the enhanced hydrolysis on the catalyst outer surface. Ion curves of m/z 18, 17 and 30 in Fig. 4b indicate the evolution of less water, roughly the same amount of ammonia and amines at a wider temperature range from PA-6,6 heated with 4A zeolite than without. These changes can be the consequence of the extended hydrolysis of amide groups diminishing the source of water evolution from polyamide.

Although enhanced hydrolysis is observed, no significant effect of heat transfer limitation has to be considered since neither the total amount of volatiles nor the temperature of the maximal rate of thermal decomposition of PA 6,6 have changed significantly with 4A zeolite. We may suppose the absence of heat transfer limitation effects also with Y zeolite of higher thermal conductivity than A zeolite [30].

3.1.2. Effect of protonic Y zeolites on the pyrolysis products of PA-6,6

In the gas chromatograms of PA-6,6 pyrolysate modified over Y type protonic zeolite displayed in Fig. 2d–f, the common feature is the dominance of aromatic and alkylaromatic hydrocarbon components. The ultrastabilized hydrogen form and the ammonium–sodium form of Y zeolite both proved to be effective denitrogenating and deoxigenating catalyst for PA-6,6 pyrolysis oil (see Fig. 2e and f). Over the calcined ammonium Y zeolite (c.NH_4NaY) of lowered hydrogen ion density less aromatic hydro-

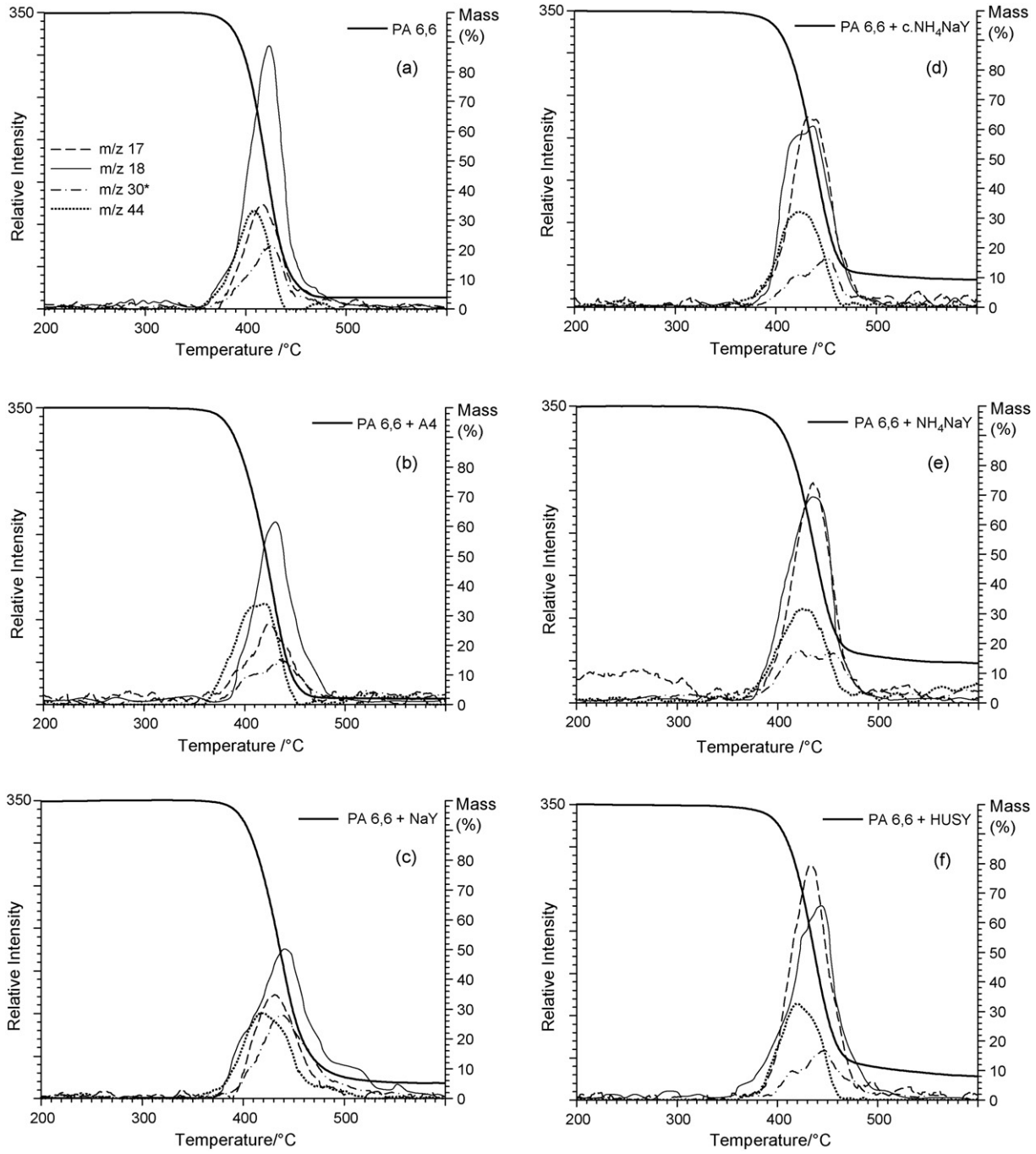

Fig. 4. TG–MS ion profiles monitored for ammonia (m/z 17), dashed line; for water (m/z 18), thin full line; for light alkylamines (m/z 30, *the intensity is multiplied by four in order to see better the ion profile), dotted-dashed line; and for carbon dioxide (m/z 44) dotted line. The corresponding TG curve is also displayed for each PA-6,6 sample heated with zeolites, thick full line.

carbons produce and several main products of PA-6,6 are still present in the chromatogram of the converted pyrolysis oil (Fig. 2d and Table 2).

Due to the catalytic activity of hydrogen Y and ammonium Y zeolites nitrogen content of the pyrolysis products of PA 6,6 is transformed at least partially into ammonia. It is known that alkylamines undergo an acid-catalyzed decomposition to alkene and ammonia on the Brønsted acid sites of Y zeolite at around 400 °C [31]. The amount of ammonia is enhanced by HUSY and NH4NaY as seen in Table 2 (peak areas at m/z 17). Amine components disappeared from the pyrolysis oil and from the highly volatile pyrolysis products as well. However, calcined ammonium Y zeolite was able only to decrease the amount of amines. In Fig. 5 the changes of the most volatile amines of 1 to 5 carbon atoms are shown by displaying mass chromatograms at m/z 30 (compare chromatograms d–f to a). This figure also indicates that amine evolution decreased while benzene formation is increased.

In the TG–MS experiments no large difference was observed between the effects of protonic Y zeolites. The TG curves obtained when PA-6,6 was heated up together with HUSY or NH_4NaY displayed in Fig. 3 nearly coincided. It is not unexpected that Y zeolites do not promote thermal decomposition of PA-6,6 since their pore

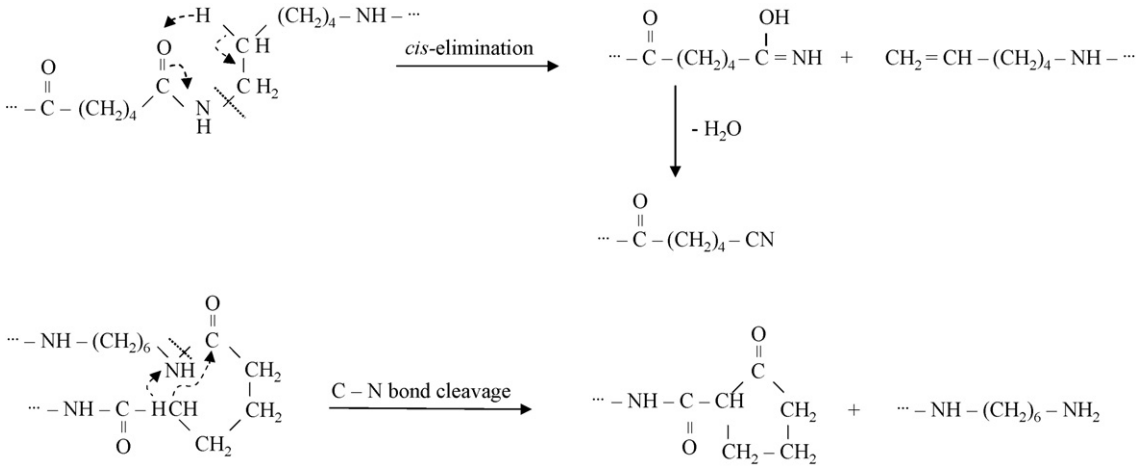

Scheme 1. Main thermal decomposition reactions of pa-6,6.

entrance is not enough wide for entering macromolecules to get in contact with the active cations inside the channels. Nevertheless, a moderate retarding effect of Y zeolites on the evolution of volatile products from PA-6,6 can be assumed that explains both the shift of the mass loss curve to 20 °C higher and the lowered decomposition rate noticed in Fig. 3. The possible effect of thermal conductivity differences of the polymer alone or heated together with zeolites can be ruled out as A zeolite has even a lower thermal conductivity than Y zeolite [30] but no delay was observed with 4A. We suppose that a certain delay of thermal decomposition of an aliphatic polyamide may be caused by the interaction of the surface of Y zeolite and the polar amide groups hindering their *cis*-elimination and intramolecular rearrangement. Comparing the TG curves in Fig. 3 we may see that the retarding effect of Y zeolites of dissimilar form is not much differing. However, the increased amount of the residual mass of polymer decomposition was different. Certainly deposited coke increases the weight of the residue by diverse extent that could be related – among other factors – to the acidity of the zeolite [32]. Carbon deposition is also observed in the pyrolysis–GC/MS experiments: the white catalyst microbed turned into black.

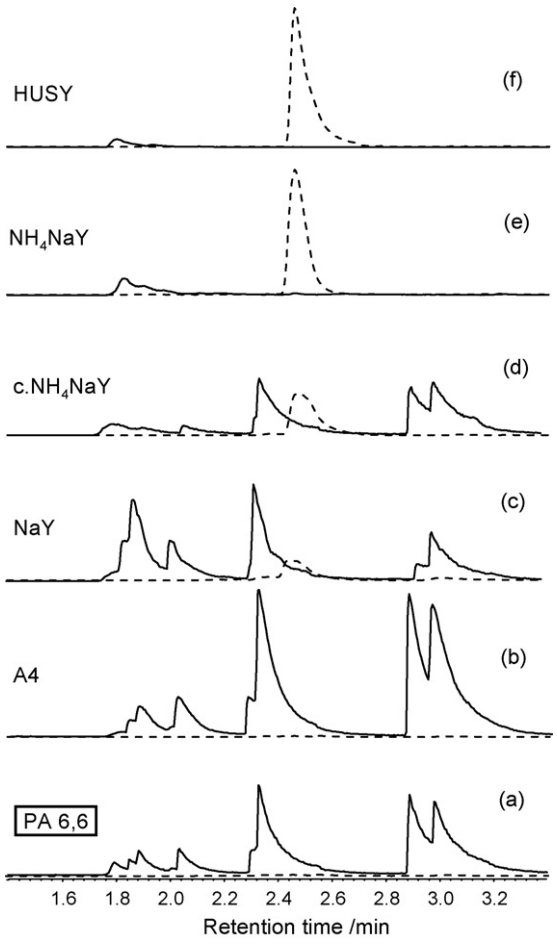

Fig. 5. GC/MS ion chromatograms of PA-6,6 highly volatile pyrolysis products obtained over the indicated zeolite, selected for tracing light alkylamines (*m*/*z* 30), full line; and benzene (*m*/*z* 78), dashed line. The intensity range is the same (count/mg polymer) for all chromatograms.

The ion curves monitored during TG experiments shown in Fig. 4d–f have similar intensity for protonic zeolites. The ion profiles of *m*/*z* 18, 30 and 44 are as wide as the corresponding curve in Fig. 4b and have similar intensity. However, we may see in these figures that the intensity of the ion curve at *m*/*z* 17 considerably increased and the mass loss curve terminated at a higher percentage when PA-6,6 is heated together with protonic zeolites. Molecular ions of benzene and toluene are also detected in the TG–MS experiments of PA-6,6 but only with protonic Y zeolites. These observations confirm the assumption that a part of the oil components of the thermal decomposition products entered into the pores of the zeolite and the nitrogen content of alkylamines is eliminated as ammonia at the same time the aliphatic hydrocarbons are converted into aromatic ones.

3.1.3. *Effect of sodium zeolite on the pyrolysis products of PA-6,6*

Fig. 2 and Table 2 show that pyrolysis products of PA-6,6 either disappear or their amounts notably decrease over NaY. Significant cracking activity of this zeolite results in the transformation of the oil components of the pyrolysate into gases, and in lower extent into new products indicated in the chromatogram c in Fig. 2. Aromatic, alkylaromatic and cyclic nitrogen-containing compounds appeared such as indanole, indene, pyridine, pyrrole, tetrahydroquinoline and their alkyl derivatives. Unsaturated linear and cyclic hydrocarbons of 2–6 carbon atoms, amines and nitriles of 2–4 carbon atoms are recognised under the large unresolved GC peak of retention time between 2 and 3 min in addition to an increased amount of carbon oxides, ammonia and water. Peaks of mass chromatogram c in Fig. 5 show that pentenyl- and pentylamine (peaks of around 3 min) decreased, but C2 and C3 amines (peaks from 1.8 to 2 min)

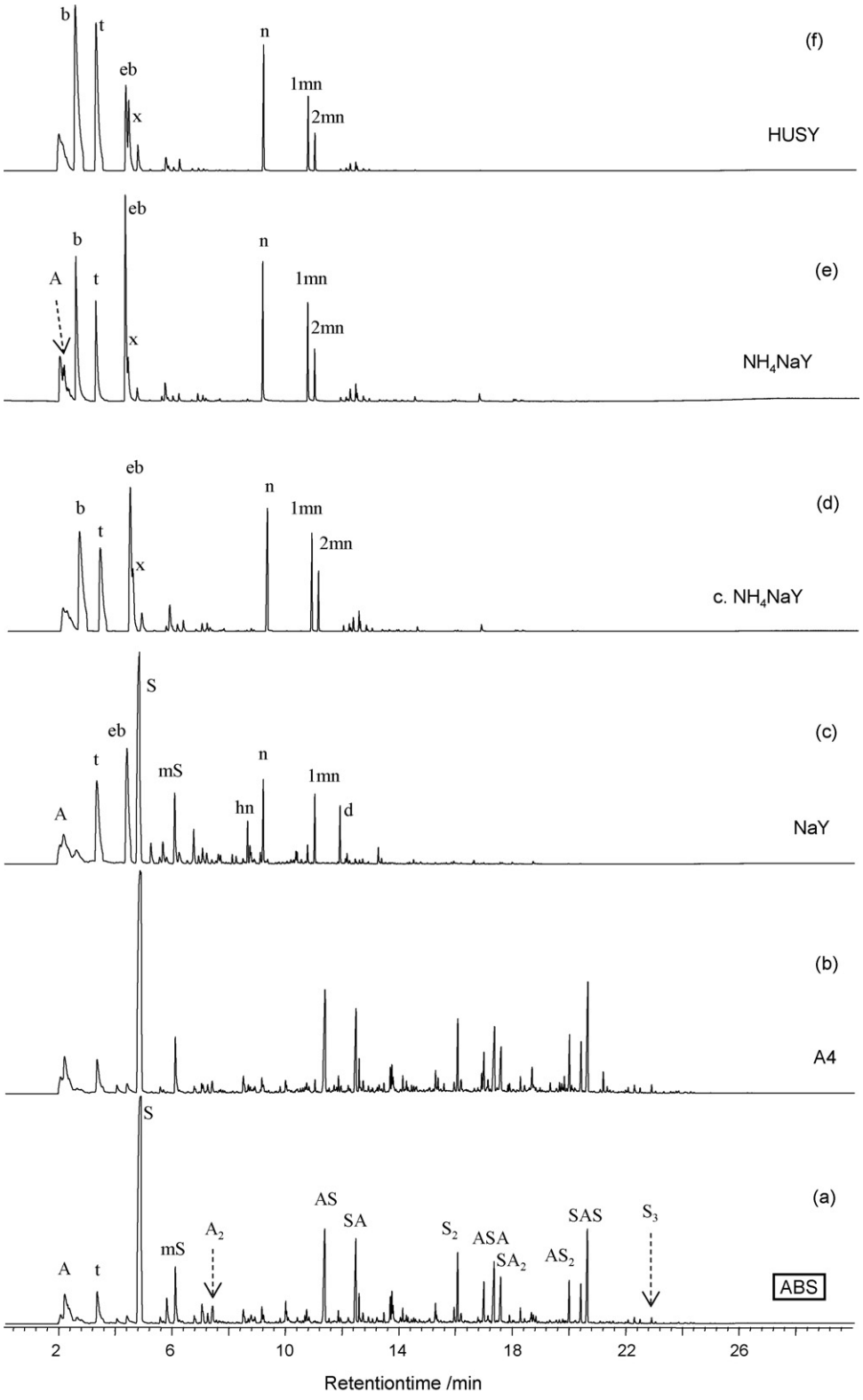

Fig. 6. Pyrolysis–gas chromatogram of ABS at 550 °C (a), and that obtained over microbed of molecular sieve 4A (b), of NaY (c), of calcined NH_4NaY (d), of NH_4NaY (e) and of HUSY (f) zeolites. The intensity range is the same (count/mg polymer) for all chromatograms. Peak annotation: b, benzene; eb, ethylbenzene; x, *o*- and *p*-xylene; hn, dihydronaphthalene; n, naphthalene; 1 mn, 1-methylnaphthalene; 2 mn, 2-methylnaphthalene; d, biphenyl; peak identities of ABS pyrolysis products (chromatogram a) are given in Table 3.

increased confirming the cracking of hydrocarbon chains by this zeolite.

TG curve of PA-6,6 with sodium Y zeolite is similar to those with protonic Y zeolites; however a lower residual mass is observed (see Fig. 3) indicating that the surface of this zeolite has similar retarding effect on the polyamide thermal decomposition while it induces lower extent of coke deposition than the protonic Y zeolites. The increased intensity of the TG–MS ion profile at *m*/*z* 30 in Fig. 4c

Table 2
GC-MS selected ion peak areas [(counts/mg) × 10^{-7}] of main pyrolysis products of PA 6,6 and that obtained over catalyst microbeds at 500 °C pyrolysis temperature

Peak[a]	Selected ion (m/z)	Catalyst					
		None	A4	NaY	c.NH_4NaY	NH_4NaY	HUSY
Gas[b]	17	0.8	0.9	1.4	1.3	9.6	1.7
Gas[b]	44	26	32	30	24	20	30
1	84	11	17	7.8	14	0	0
2	30	3.6	7.0	0.4	2.1	0	0
3	30	6.2	11	1.6	4.5	0	0
4	68	1.9	6.1	0	1.9	0.6	0
5	113	2.7	2.4	0.2	2.5	0	0
6	158	1.5	3.7	1.1	1.6	0	0
7	82	0.5	0.5	0	0.2	0	0
8	82	4.1	3.8	0	1.5	0	0
9	82	1.0	1.3	0	0.5	0	0
10	153	0.3	0.1	0	0.1	0	0
11	226	0.9	0.4	0	0.1	0	0

[a] Peak number refers to the indication in Fig. 2.
[b] First unresolved peak in the total ion chromatogram in Fig. 2.

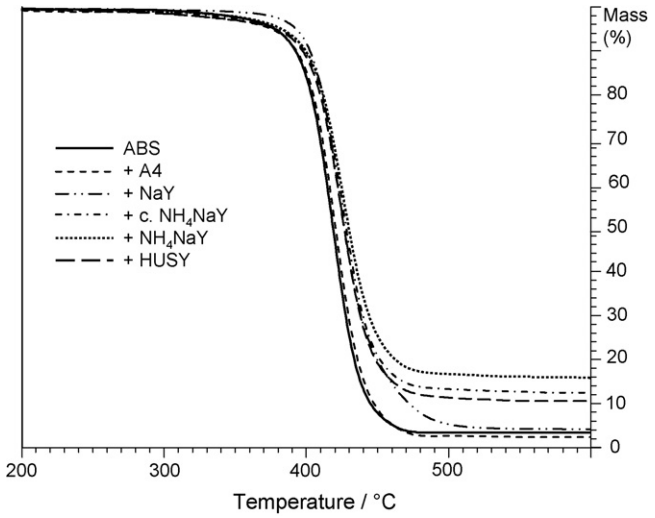

Fig. 7. Thermogravimetric analysis of ABS with zeolites. Mass loss curve of ABS, full line; ABS with 4A, short dashed line; PA-6,6 with NaY, double dotted-dashed line; PA-6,6 with calcined NH_4NaY, dotted-dashed line; PA-6,6 with NH_4NaY, dotted line; PA-6,6 with HUSY, long dashed line.

shows that a part of the thermal decomposition products of PA-6,6 are cracked into light amines. In contrast to protonic Y zeolites sodium Y is not able denitrogenate the pyrolysis oil of PA-6,6 but the less volatile components of the oils are converted mostly into gaseous compounds over this zeolite.

3.2. Acrylonitrile–butadiene–styrene copolymer

The pyrolysis–gas chromatogram of ABS displayed in Fig. 6 (chromatogram a) shows that styrene is the most significant thermal decomposition product but dimers and trimers composed of styrene and acrylonitrile monomer segments are also main components of the pyrolysis oil (listed in Table 3) in accordance with the free radical mechanism governing the pyrolysis of vinyl polymers [22,23]. Thermogravimetric analysis of ABS demonstrates that this copolymer decomposes at around 420 °C and a residue of 3% mass is left after total decomposition in an inert atmosphere (Fig. 7). In Fig. 8a TG–MS ion profiles of acrylonitrile and styrene molecular ion at m/z 53 and 104, respectively, moreover that of parent ion of toluene, ethylbenzene and xylenes at m/z 91 are nearly coinciding sharp peaks situated in the centre of the decomposition.

3.2.1. Effect of molecular sieve 4A on the pyrolysis products of ABS

Chromatogram b in Fig. 6 shows that 4A has any significant effect neither on the pyrolysate composition nor on the yield of volatile compounds evolved from ABS. The TG curve and TG–MS ion profiles of ABS heated together with 4A also hardly differs from that of ABS (see Figs. 7 and 8b).

3.2.2. Effect of protonic Y zeolites on the pyrolysis products of ABS

The pyrolysis–gas chromatogram of ABS at 550 °C changes considerably when the pyrolysis products passed over the microbed of protonic Y zeolite catalysts, as demonstrated in Fig. 6. All dimers and trimers are converted to aromatic molecules, and nitrogen-

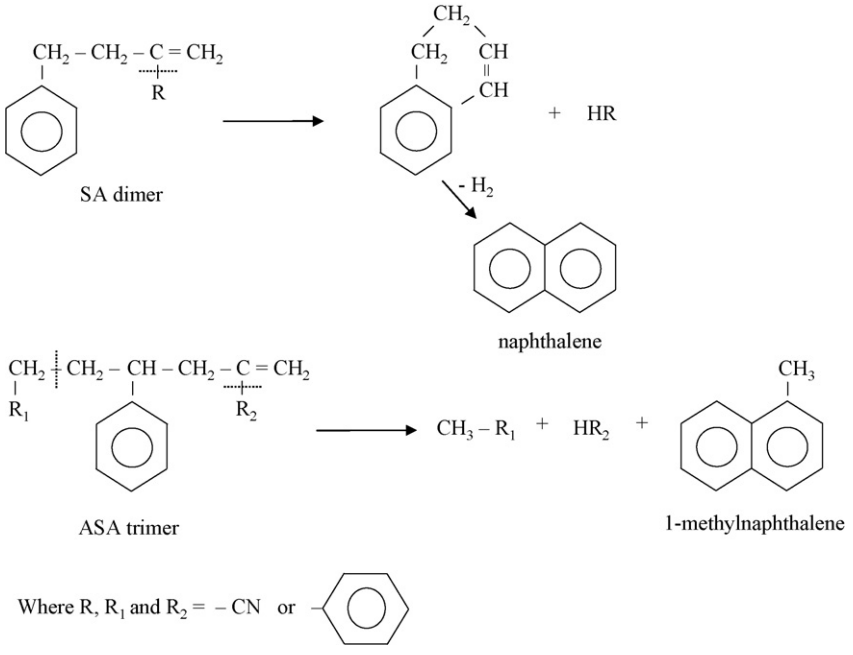

Scheme 2. Aromatization of alkenyl moieties of acrylonitrile–styrene dimer and trimer molecules.

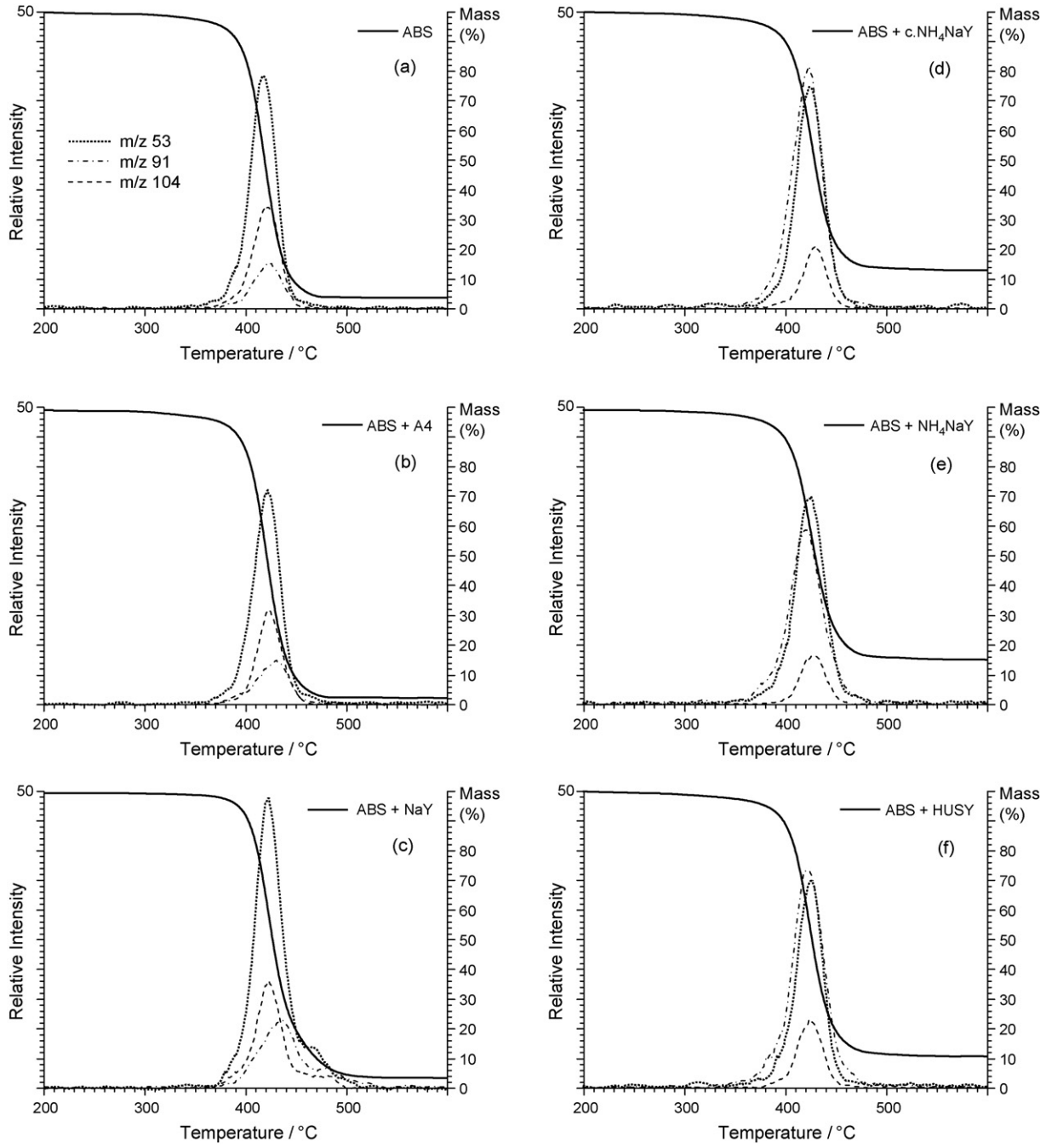

Fig. 8. TG–MS ion profiles monitored for acrylonitrile (m/z 53), dotted line; for alkylbenzenes (m/z 91), dotted-dashed line; and for styrene (m/z 104). The corresponding TG curve is also displayed for each ABS sample heated with zeolites, full line.

containing compounds do not appear in the pyrolysis oil after catalytic conversion. The oil components of conversion are benzene, naphthalene and their alkyl derivatives. We may admit that in the molecules of dimers and trimers of acrylonitrile and styrene the butenyl and hexenyl moieties are cyclized and aromatized to produce naphthalene and 1-methylnaphthalene, by eliminating a hydrogen cyanide or benzene, and additionally an acetonitrile or a toluene molecule, respectively (Scheme 2). With the help of zeolite Y the hydrogen atoms released by aromatization could be added to styrene resulting in ethylbenzene. Enhanced benzene, toluene, ethylbenzene and lesser dimer, trimer formation was also observed in polystyrene catalytic decomposition with HY zeolites in earlier works [8–10]. Moreover, we have to suppose isomerization as well to understand formation of xylenes and 2-methylnaphthalene.

The product gas is rich in nitriles, and only that obtained over ammonium form of Y zeolite contains ammonia. Mass chromatograms of the acetonitrile and acrylonitrile molecular ions at m/z 41 and 53, respectively, are displayed in Fig. 9. The figure shows that acrylonitrile is decreased but acetonitrile increased by converting ABS pyrolysis products over protonic zeolites. Note, in the mass chromatogram at m/z 41 the first peak from 2 to 2.1 min indicates unsaturated hydrocarbons, the second one at around 2.2 min corresponds to acetonitrile, while the third peak from 2.3 to 2.4 relates to the fragment ion of butenenitrile.

Table 3
Main thermal decomposition products of ABS at 550 °C

GC Peak label[a]	Compound name	*M* (Da)	Retention time (min)
A	Acrylonitrile	53	2.19
t	Toluene	92	3.32
S	Styrene	104	4.84
mS	Methylstyrene	118	6.08
A_2	2,4-Dinitrilebut-1-ene (Acrylonitrile dimer)	106	7.39
AS	2-Nitrile-4-phenylbut-1-ene	157	11.35
SA	2-Phenyl-4-nitrilebut-1-ene	157	12.44
S_2	2,4-Diphenylbut-1-ene (Styrene dimer)	208	16.03
ASA	2,6-Dinitrile-4-phenylhex-1-ene	210	17.32
SA_2	4,6-Dinitrile-2-phenylhex-1-ene	210	17.55
AS_2	2-Nitrile-4,6-diphenylhex-1-ene	261	19.96
SAS	4-Nitrile-2,6-diphenylhex-1-ene	261	20.60
S_3	2,4,6-Triphenylhex-1-ene (styrene trimer)	312	22.86

[a] Peak label refers to the indication in Fig. 6.

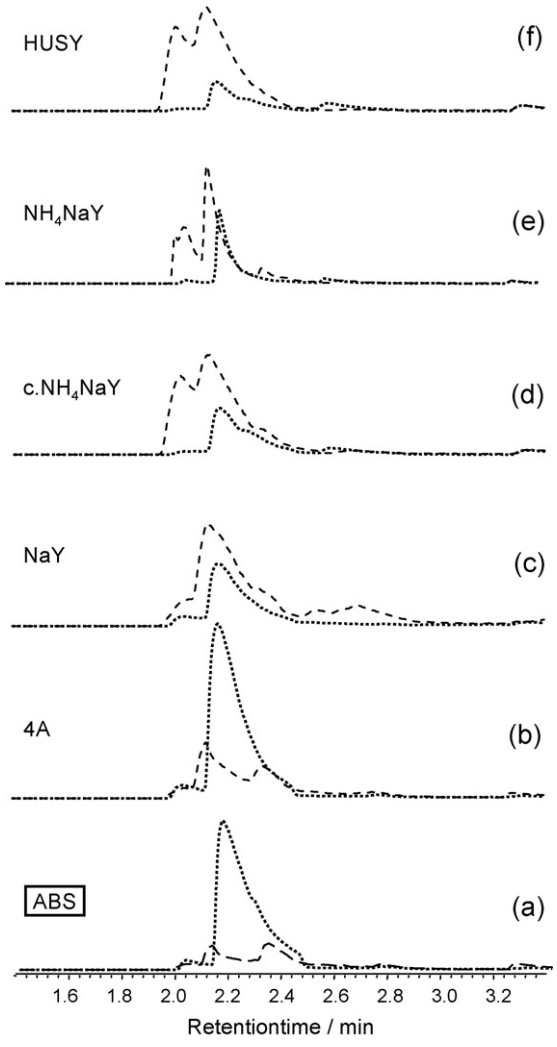

Fig. 9. GC/MS ion chromatograms of ABS highly volatile pyrolysis products obtained over the indicated zeolite, selected for tracing acrylonitrile (*m*/*z* 53), dotted line; and acetonitrile (*m*/*z* 41), dashed line. The intensity range is the same (count/mg polymer) for all chromatograms.

The TG curve of ABS is also shifted to higher temperature when heated together with Y zeolites, but this shift is only 10 °C (Fig. 7). The small retarding effect of Y zeolites in the thermal decomposition of ABS is independent of the nature of the cations, so we may suppose a minor extent of radical termination on the surface of Y zeolites. The residual mass after complete decomposition of ABS increased over 10% which effect is similar to that observed in the case of polyamide described above in Section 3.1.2, and can be explained similarly by coke deposition. The ion curves monitored during TG experiments shown in Fig. 8d–f reveals that acrylonitrile evolution (*m*/*z* 53) does not change much, but extensively more alkylbezenes (*m*/*z* 91) and less styrene (*m*/*z* 104) are produced when ABS is heated up together with protonic Y zeolites.

3.2.3. *Effect of sodium Y zeolite on the pyrolysis products of ABS*

The chromatogram c in Fig. 6 represents ABS pyrolysis oil converted over NaY zeolite that indicates also some extent of aromatization through the mechanism proposed in Scheme 2. The presence of biphenyl and dihydronaphthalene (GC peak at 8.7 min, preceding naphthalene) among the products suggests that hydrogen transfer is much less promoted over NaY than over protonic Y zeolites. The fact that styrene is converted only partially and methylstyrene remained a main component of the oil confirms the validity of this explanation. Additionally, as neither xylene nor 2-methylnaphthalene formed we may say that methylating of aromatic rings does not occur.

The TG curve of ABS when heated together with NaY is similar to those with protonic Y zeolites up to 450 °C (Fig. 7). The last stage of decomposition proceeds at a decreasing rate further on above this temperature and finishes leaving a residue of lower mass % then with protonic zeolites. The ion profiles monitored during TG–MS experiments (Fig. 8c) show that the amount of evolved acrylonitrile and alkylbenzenes slightly increases; moreover the evolution of all the three inspected components is considerably elongated with NaY zeolite at the last stage of thermal decomposition.

4. Conclusion

The majority of the volatile thermal decomposition products of polyamide-6,6 and ABS are converted over Y zeolites. The following chemical changes are observed:

- Protonic Y zeolites advance cyclization and aromatization of hydrocarbon chain segments in substituted olefins and also in aliphatic amine and amide molecules after elimination of the nitrogen-containing functional groups and substituents. Hydrogenation of styrene and methyl substitution to benzene and naphthalene rings are also catalyzed by these zeolites. Ultrastabilized hydrogen form and ammonium–sodium form Y zeolites have roughly similar activity in these reactions. But after calcination ammonium–sodium Y become considerably less effective in eliminating amino and nitrile groups that could be related to lowered Brønsted acidity.
- Sodium Y zeolite apparently cleaves C—C bonds in aliphatic amines and amides preferably compared to C—N ones, moreover strongly promotes cyclization of hydrocarbon and aliphatic amine fragments. Hydrogen elimination resulting in aromatization on one hand and hydrogenation of styrene on the other hand is much less supported by this Y zeolite than by the protonic ones.
- TG experiments revealed that the yield of solid residue of both polymers considerably increased in the presence of protonic Y zeolites that should due (at least partially) to coke deposition. A further detailed study is necessary on coke formation reactions and on the regeneration of Y zeolite deactivated in pyrolysis products conversion.

Acknowledgement

This work was supported by the Hungarian National Research Fund (OTKA) contract nos. K61504 and K68752.

References

[1] J. Scheirs, W. Kaminsky (Eds.), Feedstock Recycling and Pyrolysis of Waste Plastics, Wiley, Chichester, 2006.
[2] A.A. Garforth, S. Ali, J. Hernández-Martinez, A. Akah, Curr. Opin. Solid State Mater. Sci. 8 (2004) 415–419.
[3] A. Marcilla, A. Gómez-Siurana, S. Menargues, Thermochim. Acta 438 (2005) 155–163.
[4] J. Aguado, D.P. Serrano, G. San Miguel, J.M. Escola, J.M. Rodrígues, J. Anal. Appl. Pyrolysis 78 (2007) 153–161.
[5] B. Saha, A.K. Ghoshal, Thermochim. Acta 453 (2007) 120–127.
[6] G. San Miguel, J. Aguado, D.P. Serrano, J.M. Escola, Appl. Catal. B-Environ. 64 (2006) 209–219.
[7] C. Breen, P.M. Last, S. Taylor, P. Komadel, Thermochim. Acta 363 (2000) 93–104.
[8] G. Audisio, F. Bertini, P.L. Beltrame, P. Carniti, Polym. Degrad. Stab. 29 (1990) 191–200.
[9] S.Y. Lee, J.H. Yoon, J.R. Kim, D.W. Park, J. Anal. Appl. Pyrolysis 64 (2002) 71–83.
[10] J.W. Tae, B.S. Jang, K.H. Kim, D.W. Park, React. Kin. Catal. Lett. 84 (2005) 167–174.
[11] M. Herrera, M. Wilhelm, G. Matuschek, A. Kettrup, J. Anal. Appl. Pyrolysis 58–59 (2001) 173–188.
[12] M. Nielson, P. Jurasek, J. Hayashi, E. Furimsky, J. Anal. Appl. Pyrolysis 35 (1995) 43–51.
[13] P.T. Williams, P.A. Horne, J. Anal. Appl. Pyrol. 31 (1995) 39–61.
[14] Y. Uemichi, J. Nakamura, T. Itoh, M. Sugioka, A.A. Garforth, J. Dwyer, Ind. Eng. Chem. Res. 38 (1999) 385–390.
[15] T. Masuda, H. Kuwahara, S.R. Mukai, K. Hashimoto, Chem. Eng. Sci. 54 (1999) 2773–2779.
[16] R. van Grieken, D.P. Serrano, J. Aguado, R. Garcia, C. Rojo, J. Anal. Appl. Pyrol. 58–59 (2001) 127–142.
[17] I. Lüderwald, F. Merz, M. Rothe, Angew. Macromol. Chem. 57 (1978) 193–202.
[18] H. Ohtani, T. Nagaya, Y. Sugimura, S. Tsuge, J. Anal. Appl. Pyrolysis 4 (1982) 117–131.
[19] A. Ballisteri, D. Garozzo, M. Giuffrida, G. Impallomeni, G. Montaudo, Polym. Degrad. Stab. 23 (1988) 25–41.
[20] S.V. Levchik, E.D. Weil, M. Lewin, Polym. Int. 48 (1999) 532–557.
[21] M.A. Schaffer, E.K. Marchildon, K.B. McAuley, M.F. Cunningham, J. Macromol. Sci. Rev. Macromol. Chem. Phys. 40 (2000) 233–272.
[22] M. Blazsó, G. Várhegyi, E. Jakab, J. Anal. Appl. Pyrolysis 2 (1980) 177–185.
[23] M. Blazsó, A. in, J. Hornung, H. Seifert Schöner (Eds.), MoDeSt Workshop on Recycling of Polymeric Materials, B3, Forschungzentrum Karlsruhe GmbH, Karlsruhe, 2004, pp. 1–7.
[24] S. Czernik, C.C. Elam, R.J. Evans, R.R. Meglen, L. Moens, K. Tatsumoto, J. Anal. Appl. Pyrolysis 46 (1998) 51–64.
[25] M. Brebu, M.A. Uddin, A. Muto, Y. Sakata, C. Vasile, J. Anal. Appl. Pyrolysis 63 (2002) 43–57.
[26] D. Ferdous, A.K. Dalai, J. Adjaye, Appl. Catal. A: Gen. 260 (2004) 137–151.
[27] Z. Sarbak, M. Lewandowski, Appl. Catal. A: Gen. 208 (2001) 317–321.
[28] M. Blazsó, J. Anal. Appl. Pyrolysis 74 (2005) 344–352.
[29] J.H.C. van Hooff, J.W. Roelofsen, in: H. van Bekkum, E.M. Flanigen, J.C. Jansen (Eds.), Introduction to Zeolite Science and Practice, Elsevier, Amsterdam, 1991, pp. 241–283.
[30] A.J.H. McGaughey, M. Kaviany, Int. J. Heat Mass Transfer 47 (2004) 1799–1816.
[31] T.L.M. Maesen, E.P. Hertzenberg, J. Catal. 182 (1999) 270–273.
[32] H.G. Karge, in: H. van Bekkum, E.M. Flanigen, J.C. Jansen (Eds.), Introduction to Zeolite Science and Practice, Elsevier, Amsterdam, 1991, pp. 531–566.